Aging effects in pentacene thin-film transistors: Analysis of the density of states modification

F. De Angelis,[a] S. Cipolloni, L. Mariucci, and G. Fortunato
IFN-CNR, Via Cinto Romano 42, 00156 Rome, Italy

(Received 9 August 2005; accepted 17 April 2006; published online 11 May 2006)

Field effect analysis has been employed in order to calculate the density of states of high quality pentacene thin-film transistors. The degradation of the electrical characteristics caused by the exposure to air has been studied and discussed in term of density of states modification. The calculated density of the states has been approximated by two exponential terms, as in amorphous silicon, and it has been used in a two-dimensional numerical simulation in order to reproduce the electrical characteristic variation with respect of the temperature and aging time. © *2006 American Institute of Physics*. [DOI: 10.1063/1.2203742]

In the last years organic thin-film transistors (OTFTs) have attracted a certain attention thanks to their interesting features such as low cost, low temperature processing, and mechanical flexibility. At present, best results have been demonstrated for pentacene-based OTFTs, obtained on a variety of substrates (silicon, aluminum, or plastic[1–4]) and dielectric layers [SiO_2 poly vinyl phenol (PVP), polyimide, poly(methyl methacrylate)[1–4] (PMMA)]. To optimize the device characteristics of OTFTs it is very important to understand the transport mechanism and how they depend on the operating environment. In fact, many problems related to the understanding of the transport phenomena[5,6] and the aging effects of the organic semiconductor[6,7] are still open. Exposure to air is, in general, detrimental to the performance of the OTFTs (Ref. 7) and the solution of this problem is one of the main issues.

In this work we present an experimental study of the aging effects on the electrical characteristics of high quality pentacene-based OTFTs. Then, using the field effect analysis of the characteristics, we discuss the device degradation in terms of modifications of the pentacene density of states.

Top contact (TC) devices have been fabricated on heavily doped silicon wafers (acting as gate electrode), with thermal silicon oxide 60 nm thick (gate dielectric). Source and drain gold contacts are defined on the top of active pentacene layer using a shadow mask ($W=200$ μm, $L=100$ μm). A thin film of PMMA (about 15 nm) has been used as a buffer layer, in order to improve the quality of the polycrystalline pentacene; a more detailed description of the fabrication process is given in our earlier work.[1]

The devices have been kept under vacuum for 60 h, and no significant aging effects have been observed. Afterward, the sample has been exposed to air and light for more than six weeks, and has been repeatedly measured as a function of the exposure time, in vacuum, nitrogen, and air: a representative group of transfer characteristics measured in vacuum at low drain voltage $V_d=-1$ V, for different aging times, is shown in Fig. 1. The as-fabricated devices exhibit a field effect mobility $\mu_{FE}=1.2$ cm^2/V s, subthreshold slope of 0.6 V/decade and threshold voltage $V_{th}=-6$ V, and on/off current ratio $I_{on/off}=10^7$ in vacuum. By analyzing the curves several observations can be pointed out: in the considered period, the aging phenomenon does not affect the subthreshold region, but it reduces the on current while the off current tends to increase with the aging time; the rate of the degradation process tends to decrease with time; the characteristics measured in nitrogen are the same to those measured in vacuum, whereas the characteristics measured in air show a little degradation of the on region.

To better understand the correlation between the aging and the transport properties, we have calculated the defect density in the pentacene film using field effect analysis. In fact, it has been shown recently that transport in pentacene TFTs can be analyzed considering localized density of states (DOS) in the band gap,[5] similar to what has been reported for amorphous and polycrystalline silicon.[8,9] In particular, we applied on pentacene TFTs the temperature method,[10,11] a very accurate technique, already applied to both amorphous and polycrystalline silicon, to calculate the DOS. It should be to pointed out that, as for polycrystalline silicon,[9] the calculated DOS must be considered as an effective DOS, including the contributions to localized states of the in-grain and grain boundary defects as well as of the dielectric/pentacene interface defects.

The transfer characteristics have been measured at different temperatures in the range $T=200-320$ K for the as-fabricated devices (shown in Fig. 2), and after 40 days aging. According to the temperature method the DOS can be ex-

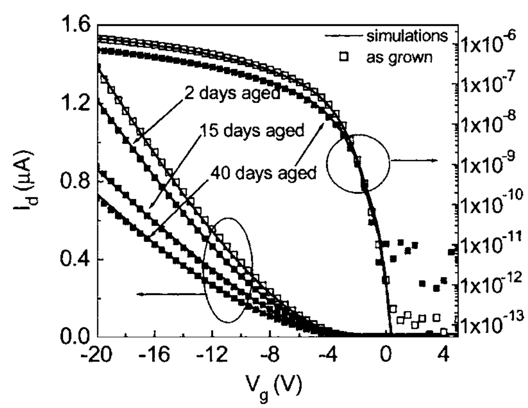

FIG. 1. Simulated (lines) and experimental transfer characteristics, measured in vacuum at $V_{ds}=-1$ V, of the as-fabricated devices (open symbols) and the devices aged (closed symbols) for 2–40 days ($L=100$ μm, $W=200$ μm, oxide thickness of 60 nm, and PMMA thickness of 15 nm).

[a]Electronic mail: mariucci@ifn.cnr.it

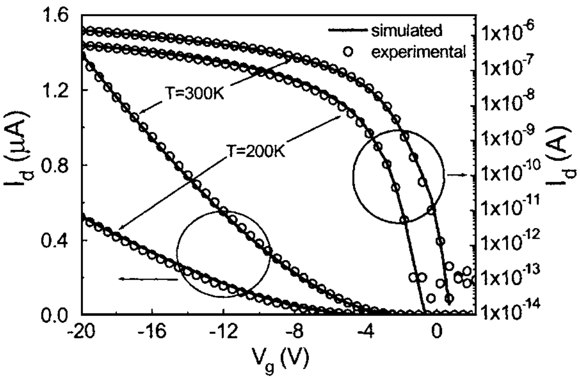

FIG. 2. Simulated and experimental transfer characteristics (measured in vacuum at $V_d = -1$ V) of the as-fabricated devices for two different temperatures (200 K, 300 K).

tracted from the normalized sheet conductance $G' = G\mu_{FE}(300\text{ K})/\mu_{FE}(T)$, where $G = I_d/V_{ds}$ is the sheet conductance which can be deduced from the I_d-V_g characteristics measured at different temperatures,[11] and $\mu_{FE}(T)$ is the temperature dependent field effect mobility, shown in Fig. 3, for both as-fabricated and aged devices. The extracted density of donorlike states for the as-fabricated device and after 40 days aging are reported in Fig. 4. According to these data, the aged devices exhibit an increase of the tail states, which is responsible for the degradation of the on region of the characteristics. On the contrary, the deep states, which control the subthreshold region, remain nearly unaffected by the aging. As in the case of polysilicon, the DOS can be reasonably approximated by the sum of two exponential terms (tail states and deep states): $N(E) = N_t e^{(-E/E_t)} + N_d e^{(-E/E_d)}$, where E is the energy, measured from the top of the valence band, E_t and E_d are the characteristics energies for the tail-state and deep-state DOS, respectively, and N_t and N_d are the tail-state and deep-state DOS values at $E=0$, respectively. The approximated DOS was then used in the two-dimensional (2D) numerical device analysis program DESSIS[12] to simulate, using the conventional drift-diffusion transport model, the transfer and the output characteristics at different temperatures and aging times. The values of the main parameters of

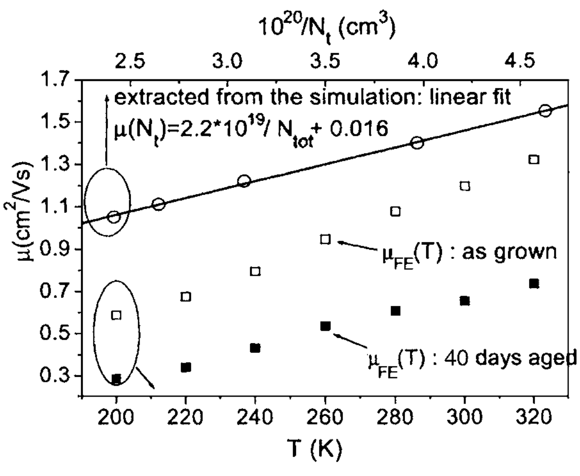

FIG. 3. Experimental values of field effect mobility $\mu_{FE}(T)$ extracted from the transfer characteristics ($V_d = -1$ V) for the as-fabricated devices (open squares) and the devices aged for 40 days (closed squares). Also shown are the values of the band mobility as a function of traps density (top axis) used in the simulations to reproduce the aging effect (open circles) and the linear fit of the data (line).

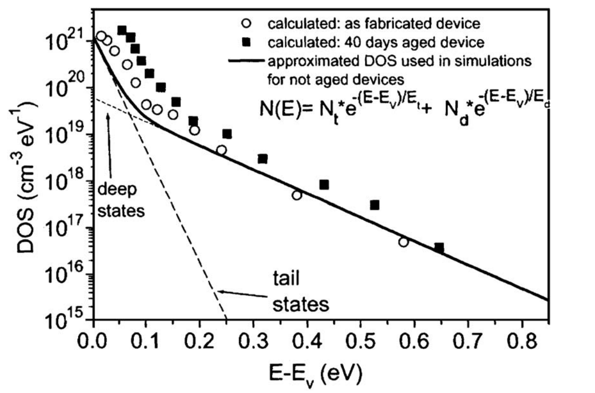

FIG. 4. DOS calculated with temperature method for as-fabricated devices (open circles) and for the device aged for 40 days (closed squares). The approximated DOS used for the simulations of the as-fabricated device (line) is also shown.

pentacene used in the simulations are reported in Table I.[5,13] The effective density of valence band states N_v was estimated assuming a square root energy distribution of the valence band density of states around the top and an effective hole mass equal to 1 electron mass.[5] The simulations of the as-fabricated device have been performed for all measured temperatures (from 200 to 320 K), including the temperature variation of $\mu_{FE}(T)$, according to the data shown in Fig. 3. A very good agreement between simulations and experimental data was found at all temperatures and the simulated characteristics are compared to the experimental data in Fig. 2 for two specific temperatures, $T=200$ K and $T=300$ K. This result confirms that the choice of the main parameters and of the transport model used (drift diffusion with a constant carrier mobility) is appropriate and represents an additional validation of the DOS distribution extracted from the temperature method. The simulated characteristics of the device aged for different times compare also very well with the experimental data reported in Fig. 1. The aged characteristics were simulated only by increasing the tail-state density and decreasing the mobility. In fact, an important result of the simulations shown in Fig. 1 is to show that the increase of the tail distribution is not sufficient to fully reproduce the aged characteristics and a proportional decrease of the band mobility is also necessary, as shown in Fig. 3. This fact is not surprising, because a gradual increase of the defect density must correspond to a gradual increase of the scattering phenomena and, hence, a decrease of the mobility.[14] According to Fig. 3, the progressive aging of the devices induces a mobility degradation that can be related to the total density of tail states N_{tot} obtained by integrating the tail term of the exponential distribution with respect to the energy E. In par-

TABLE I. Parameters used in 2D simulations of devices not aged and aged for 40 days.

Parameter	As grown	40 days aged
Energy gap (eV)	2.4	2.4
Refractive Index	2	2
Work function (eV)	5.0	5.0
Effective density of the states N_v (cm^{-3})	3×10^{19}	3×10^{19}
Band mobility (cm^2/V s)	1.55	1.05
N_t(cm^{-3})/E_t (meV) (tail states)	$1.2\times10^{21}/17$	$2.2\times10^{21}/17$
N_d(cm^{-3})/E_d (meV) (deep states)	$6\times10^{19}/85$	$6\times10^{19}/85$

ticular, we found that the band mobility after aging, μ', can be approximated by the following relationship: $\mu' = \mu N_{tot}/N_{tot}'$ where N_{tot}' is the total tail-state density after aging. The other parameters (deep-state DOS, energy gap, work function, etc.) used in the simulations of aged devices were unchanged. As a consequence, an increase of mobility of pentacene TFTs can be achieved by a reduction of tail states, obtained by improving device preparation.

Recent works have shown that adsorbed oxygen and/or water are probable origin of the defects in pentacene films observed by deep level transient spectroscopy (DLTS) measurements.[5,14] In addition, numerical calculation confirmed[15] that oxygen atoms, included in pentacene molecules, induce defects levels near the valence band. Then, we suggest that the tail-state density increase, induced by aging process and measured by field effect, is related to the oxidation of pentacene film, caused by humidity or oxygen contained in air.

In summary, we have fabricated high quality pentacene OTFTs in top contact configuration and we have studied the variation of their electrical characteristics induced by the aging time. The temperature method has been successfully applied for the determination of pentacene DOS, both for as-deposited and aged devices, showing that device degradation induced by aging can be related to an increase tail-state density as well as to a field effect mobility reduction. The calculated DOS has been also used in 2D numerical simulations performed with the program DESSIS and a very good reproduction of the experimental data has been obtained at different temperatures as well as for different aging times. It should be also pointed out that, in order to best fit the experimental data with the 2D numerical simulations, a dependence of the field effect mobility on the total amount of tail states (μ=const/N_{tot}) must be introduced. Finally, we have suggested that aging effects could be related to pentacene oxidation that induces additional tail states with a consequent field effect mobility degradation.

This work was supported by the project MICROPOLIS, under the program FIRB funded by Italian ministry of Education University and Research (MIUR).

[1]F. De Angelis, S. Cipolloni, L. Mariucci, and G. Fortunato, Appl. Phys. Lett. **86**, 203505 (2005).
[2]H. Klauk, M. Halik, U. Zschieschang, G. Schimd, W. Radik, and W. Weber, J. Appl. Phys. **92**, 5259 (2002).
[3]S. Pyo, H. Son, K. Choi, and M. H. Yi, Appl. Phys. Lett. **86**, 133508 (2005).
[4]Y. Jin, Z. Rang, M. I. Nathan, P. P. Ruden, C. R. Newman, and D. Frisbie, Appl. Phys. Lett. **85**, 4406 (2004).
[5]A. R. Volkel, R. A. Street, and D. Knipp, Phys. Rev. B **66**, 195336 (2002).
[6]Y. Suk Yang, S. H. Kim, J. Lee, H. Y. Chu, L. Do, H. Lee, J. Oh, T. Zyung, M. K. Ryu, and M. S. Jang, Appl. Phys. Lett. **80**, 1595 (2002).
[7]C. R. Kagan, A. Afzali, and T. O. Graham, Appl. Phys. Lett. **86**, 193505 (2005).
[8]M. Shur and M. Hack, J. Appl. Phys. **55**, 3831 (1984).
[9]G. Fortunato and P. Migliorato, Appl. Phys. Lett. **49**, 1025 (1986).
[10]G. Fortunato, D. B. Meakin, P. Migliorato, and P. G. Le Comber, Philos. Mag. B **57**, 5 (1988).
[11]V. Foglietti, L. Mariucci, and G. Fortunato, J. Appl. Phys. **85**, 616 (1999).
[12]*DESSIS Users Manual Release 6* (ISE Integrated System Engineering, Zurich, Switzerland, 1999); www.ise.ch/products/dessis
[13]T. Li, J. W. Balk, P. P. Ruden, I. H. Campbell, and D. L. Smith, J. Appl. Phys. **91**, 4312 (2002).
[14]Oana D. Jurchescu, J. Baas, and T. T. M. Palstra, Appl. Phys. Lett. **84**, 3061 (2004).
[15]J. E. Northrup and M. L. Chabinye, Phys. Rev. B **68**, 041202(R) (2003).